

Experimental Investigation Study into the Mechanical Properties of Autoclaved Aerated Concrete and Its Bond Material

Sarra'a Dhiya'a Jaafer , Ashraf A. Alfeehan* 

Civil Engineering Department, College of Engineering, Mustansiriya University, Baghdad, Iraq

*Email: drce_ashrafalfeehan@uomustansiriyah.edu.iq

Article Info

Received 01/02/2024

Revised 27/03/2025

Accepted 03/04/2025

Abstract

Most mechanical properties are often required for the design and linear or nonlinear modeling of masonry structures, as well as performance-based design. This article presents an experimental evaluation of the mechanical properties of autoclaved aerated concrete AAC masonry blocks and common bonding and plastering materials. The tests covered the most important mechanical properties of the materials, including density, compressive strength, tensile strength, flexural strength, modulus of elasticity, Poisson's ratio, and shear bond. Samples of AAC blocks were prepared and tested, in addition to three typical materials utilized with these blocks: cement-sand, gypsum, and adhesive mortars. The shear bond test as triplet prisms was conducted to estimate the AAC block and bond material shear strengths. The results showed that cement-sand mortar was superior to other bonding materials in compressive strength. In contrast, the adhesive mortar showed higher tensile and shear strength values due to its special composition, which gives greater adhesive forces between different materials.

Keywords: Autoclaved aerated concrete; Masonry; Mechanical properties; Mortar material; Push test

1. Introduction

Since the early 1900s, autoclaved aerated concrete, or AAC, has been manufactured on an industrial scale for use in construction, and it is a type of precast concrete material with a low density and excellent insulation properties such as thermal insulation and sound absorption qualities. AAC is steam-cured and is practically stable; it is a form of very lightweight concrete produced by closed, uniformly distributed air bubbles; it is formed of sand that can be replaced partially or entirely with fly ash, water, gypsum, cement, lime, and aluminum powder as an expansion agent. The low density is achieved by forming air voids to produce a cellular structure; the low density of AAC block performs well for low-to-medium-rise building cladding, infills, and bearing wall components. In addition, due to its high thermal conductivity, it can offer excellent fire-rating qualities and affordable design options for low-energy structures. Its interior porosity contributes to its extremely low sound transmission, producing an exceptionally effective acoustically for a material of its weight. It's easy and flexible to manufacture AAC with special specifications such as product characteristics, shape, and size; it has a wide range of forms and sizes [1]. The structural use of AAC as an AAC wall and floor panel [2]. For masonry buildings to resist lateral or eccentric loads and in-

plane forces acting parallel to the wall's plane, the bond strength between the brick and mortar is crucial. This bond strength has an impact on the shear strengths of these walls. Various factors such as mortar types, surface features, frog size and form, block water absorption, curing technique, and craftsmanship can affect the strength of the connection between the block and mortar [3]-[5]. Many variables about the properties of masonry units and mortar, such as the block's moisture content, water absorption, and bonding surface roughness, affect how the masonry unit-mortar connection develops. The workability, composition, and water retention capacity of mortar are important characteristics. Several investigations have been conducted on the bond strength of masonry [6]. Thamboo et al. found that textured units with smooth surfaces had stronger shear bonds than those with rough surfaces. Thamboo et al. revealed that, compared to wet-cured specimens, dry-cured thin-layer mortar masonry specimens have better bond strength and Young's modulus [7]. Shear strength may be determined using two distinct test methods in the context of seismic design for new masonry constructions: diagonal compression and shear triplets. The results show that the triplet test is more useful than diagonal compression because it is simple and provides accurate results [8]. Barrattucci et al. [9] conducted triplet experiments on masonry units exposed to cyclic and monotonic

shear loadings with varying cement percentages. Regardless of the mortar composition, triplet shear tests showed that cyclic loading considerably reduces the peak shear strength (normally about 18%) in comparison to monotonic loads.

Sarangapani et al. [10] applied an effort to find out how the relationship between brick and mortar develops. They demonstrated that the network of cement hydration products deposited inside the brick pores and on the brick surface creates the brick-mortar interaction. The brick-and-mortar bond is mainly mechanical. Basha represented the impact of kinds of structural bonding on the mechanical properties of masonry subjected to shear, flexure, and compression loads using the DIC approach in studies conducted on masonry. Full-brick thick masonry was shown to have greater capacity and deformation properties than half-brick thick masonry. Full-brick thick Flemish bond prisms exhibited more deformable behavior and greater compressive strength and related strain than half-brick thick masonry prisms; the rupture modulus of the Flemish bond masonry walls was four times greater to stack bond masonry. Because the bond arrangement prevented diagonal rupture propagation, the diagonal compression strength of full-brick thick masonry wallets was about 1.3 times greater than that of running bond wallets. Structural bonding patterns must be carefully considered when evaluating the mechanical properties of masonry that are necessary for the design and analytical modeling of masonry projects [11]. A significant effort has been devoted to previous research to study the behavior of shear bond strength for AAC masonry. Still, the effect of mortar type and mechanical properties of AAC block and mortar on bond strength has not been clarified. This study attempts to give a clearer picture of the shear bond strength of AAC masonry using several mortar types. It investigates how

the mechanical properties of each mortar type and AAC block affect the behavior of the shear bond.

2. Research Significance

Because AAC blocks have evolved from partition walls to load-bearing walls, more research is needed to understand the mechanical properties of AAC blocks and their bonding materials under distributed loading conditions. This will help provide a clear picture of the behavior of walls constructed with these blocks. Density, compressive strength, tensile strength, modulus of rupture, Poisson's ratio, and modulus of elasticity tests were conducted to achieve this. The shear bond strength of the block and mortar joint was evaluated using shear testing. The shear strength and other mechanical properties are often required for linear and nonlinear modeling of masonry structures and performance-based design.

3. Experimental Program

The experimental study on the mechanical properties of AAC blocks and three types of bonding materials, including cement and sand mortar, gypsum mortar, and adhesive material mortar, has been carried out by conducting standard tests that reflect the general behavior of the AAC wall. In addition, these properties are essential for material modeling in finite element software applications. The work covered preparing the required samples of the AAC blocks and their bonding materials to conduct the required tests. The properties of AAC blocks and the bonding materials were evaluated, as shown in Table 1.

Table 1. Tests of AAC Blocks and the Bonding Materials

Material	Test	No. of specimens	Dimensions (mm)	Specification
AAC Blocks	Density	3 cubes	100×100×100	ASTM C1386
	Compressive strength	3 cubes	100×100×100	ASTM C1386
	Tensile strength	3 8-shape	-	ASTM C307
	Modulus of Rupture	3 prisms	100×100×300	ASTM-C78
	Dynamic elasticity	3 prisms	100×100×300	ASTM C-215
	Ultrasonic pulse	3 prisms	100×100×300	ASTM, 1990. D 2845-90
	Dynamic Poisson's ratio	3 prisms	100×100×300	ASTM C-215
	Density	3 cubes	50×50×50	ASTM C138
Mortar	Compressive strength	3 cylinders	50×100	ASTM C109
	Direct tensile strength	3 8-shape	-	ASTM C307
	Indirect tensile strength	3 cylinders	50×100	ASTM C496/C496-04
	Modulus of Rupture	3 prisms	40×40×160	ASTM C348-21
	Dynamic elasticity	3 prisms	40×40×160	ASTM C-215
	Ultrasonic pulse	3 prisms	40×40×160	ASTM, 1990. D 2845-90
	Dynamic Poisson's ratio	3 prisms	40×40×160	ASTM C-215

The work extended to perform a direct shear test. Each specimen for a direct shear test was created by preparing and connecting three cubes made of AAC block by using a specific type of bonding material.

3.1 Bonding Materials

Three types of bonding materials were used in this work: cement and sand mortar, gypsum mortar, and adhesive mortar. The chemical components for materials are listed in Table 2 unless the adhesive was not tested and the characteristics according to the source. The physical properties of cement, sand, and gypsum are listed in Tables 3, 4, and 5. The percentage of the mortar mix was one cement unit to 3 sand units by weight with a 0.6 water-to-cement ratio to provide suitable workability according to realistic working conditions. The cementitious samples were cured in water at approximately 25°C. The gypsum mortar was prepared according to Iraqi specifications using water/gypsum with a ratio of 1:3 by weight. The mix components optimized of adhesive material mortar were 1:3 adhesive powder to water by weight. The gypsum and adhesive mix took about one minute to attain the required homogeneity and workability, but the cement-sand mortar took about three minutes.

Table 2. Chemical Specification of Materials

Chemical Composition	Percentage by Weight		
	Cement	Gypsum	Sand
CaO	60.9	18.86	0.7
SiO ₂	21.86	23	97.5
AL ₂ O ₃	4.4	20	2.76
Fe ₂ O ₃	3.61	20	0.4
MgO	2.25	5.75	0.7
SO ₃	2.61	-	-
Na ₃ O	-	0.03	-
K ₂ O	-	1.47	-
Cl	-	0.026	-
L.O.I	2.43	-	1
I.R.	0.96	-	-
L.S.F	0.98	-	-

Table 3. Physical Properties of Cement

Physical Properties	Results
Specific surface area (blain method), m ² /kg	352
Setting time (Yicale's method)	
The initial setting, hrs: min	2:35
The final setting, hrs: min	5:20
Auto-calve expansion%	0.24

Table 4. Physical Properties of Sand

Physical Properties	Test Results
Specific Gravity	2.63
Absorption	0.65%
Sulfate Content	0.34%

Table 5. Physical Properties of Gypsum

Physical Properties	Test Results
Specific Gravity	2.31
fineness	5
Setting time	14

Fig. 1 shows each mix of the bonding material.

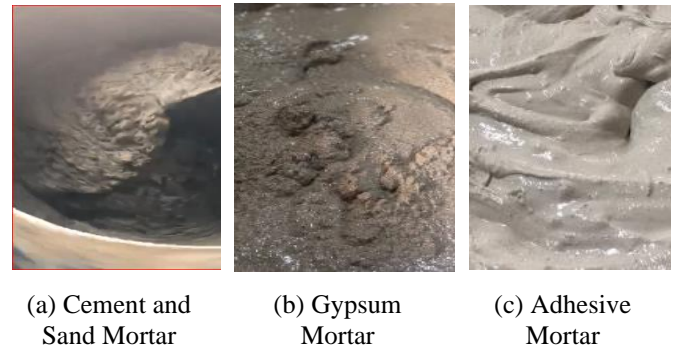


Figure 1. Bonding Materials Mix

3.2 Density of AAC

Density is related to w/c ratio, compatibility, porosity, and pore size distribution [12]. The range of the dry density of AAC as described in RILEM Recommendation AAC 4.1 is (200-1000) kg/m³, while RILEM (1993) states that the density range for AAC is (300-1800) kg/m³. Also, Schober (2005) states that the range is (100-800) kg/m³ [12]-[13].

The density testing was done using cubic specimens 100 mm cut from the main block. They were used to estimate the density by weighing these cubes in dry states after the specimens were dried to a constant mass. The average of three specimens has been used to evaluate the density of the AAC block. The equation used to determine the density is:

$$\gamma = \text{weight}/\text{volume} \quad (1)$$

3.3 Mechanical Properties of AAC

The preparation of test samples and the test methods of mechanical properties were described. The mechanical properties of AAC are compressive strength, modulus of elasticity, tensile strength, modulus of rupture, ultrasonic pulse velocity, and Poisson's ratio. The average of three specimens has been used to evaluate the mechanical properties [14]-[18].

3.3.1 Compressive Strength f'_c

Compressive strength was measured using destructive and non-destructive methods. The destructive test used cubic specimens (100) mm to estimate the compressive strength, as shown in Fig. 2. The density and porosity of AAC significantly impact its compressive strength. The compressive strength diminishes as porosity increases and density decreases [15]. Table 6 shows the ASTM Specification C1693-11 AAC [16].

Table 6. ASTM Specification C1693-11 AAC [16]

Strength Class	Min Compressive Strength (MPa)	Nominal Dry Bulk Density (kg/m ³)	Density Limits (kg/m ³)
AAC-2	2	400-500	350 550
AAC-3	3	500-600	450 650
AAC-4	4	500-600	450 650
AAC-5	5	600-700	550 750
AAC-6	6	600-700	550 750



Figure 2. Compressive Strength Test for Autoclaved Aerated Concrete Cubic Specimens

The compressive strength of AAC blocks is determined according to ASTM C1386.

The equation used to calculate the compressive strength is:

$$f'_c = P/A \tag{2}$$

where: f'_c : compressive strength (MPa),

P : applied load (N),

A : area of the surface (mm²)

The non-destructive method was done by using ultrasonic pulse velocity measurements (UPV) [17], as shown in Fig. 3. In this procedure, the specimen receives an impulse, and the amount of time needed for the ultrasonic waves to travel through the specimen's smallest cross-section is then measured. The ultrasonic pulse velocity of the waves is measured directly and obtained in the monitor. The following equation is used to calculate the value of f'_c :

$$C: 2.016 e^{0.61 D} \tag{3}$$

Where:

C : compressive strength (MPa),

D : direct ultrasonic velocity (km/sec),

e : exponential factor.

3.3.2 Tensile Strength f_t

A direct tensile strength test was done for the AAC block using an eight-shape specimen. Valore (1954b) stated that AAC's direct tensile strength to compressive strength



Figure 3. Ultrasonic Machine and Test

The ratio is between (0.15-0.35), whereas Legatski stated the ratio is between (0.1-0.15) [10]. The machine of tensile strength was used in this test, as shown in Fig. 4. The specimen was placed inside a steel mold of 8 shape and closed tightly. Then, the specimens are subjected to a tensile load using two arms connected to the steel molds until the specimen fails and splits into two pieces. Equation 4 has been proposed to predict AAC's tensile strength based on ASTM C307[18],[20]-,[21].

$$f_t = 2.4 \sqrt{f'_{AAC}} \tag{4}$$

where: f'_{AAC} : compressive strength of AAC block (psi).



Figure 4. Tensile Test Machine

3.3.3 Modulus of Flexural (Modulus of Rupture) f_r

A flexural strength test was done using three

AAC blocks with dimensions (100×100×600) mm are shown in Fig. 5. The blocks were tested with two-point loads, with a distance between the point loads of 150 mm, and the prism was placed on two supports with a distance between them of 450 mm according to ASTM-C78. Valore (1954b) states that the flexural strength ratio is about (0.22-0.27)% from compressive strength and nearly zero for very low-density AAC [12].

The equation calculates the flexural strength:

$$f_r = \frac{Pl}{bd^2} \quad (5)$$

where:

f_r = modulus of rupture (MPa)

P = failure load (N)

l = span length between center to center of supports (mm)

d = depth of specimen cross section (mm)

b = width of specimen cross section (mm)

Also, the modulus of rupture can be estimated using the recommended practice of Equation of RILEM. Autoclaved aerated concrete from [12],[20]:



Figure 5. Flexural Test for AAC Prism

$$MOR = 0.27 + 0.21f_{ct} \quad (6)$$

Where:

MOR : modulus of rupture (MPa)

f_{ct} : compressive strength (MPa)

Also, the flexural strength of AAC can be calculated using the equations below [19]:

$$f_{flk} = 0.18 f_{ck} \quad (7)$$

Where: f_{flk} : flexural strength of AAC,

f_{ck} : compressive strength of AAC

3.3.4 Modulus of Elasticity

Timoshenko (1970) defined the modulus of elasticity as the ratio of (stress/strain) [10]. AAC modulus of elasticity (E_c) values are related to dry density and compressive strength. The

modulus of elasticity (E_c) of AAC block specimens was done using non-destructive test equipment (NDT James Instruments), as shown in Fig. 6.

Because the samples are precast and due to the difficulty of forming them to the required measurements, it was sufficient to conduct dynamic tests for the modulus of elasticity and Poisson's ratio. Using longitudinal frequency mode test to calculate the dynamic modulus of elasticity by using the following equation [22]:

$$E = DM(n')^2 \quad (8)$$

Where:

E : Dynamic modulus of elasticity

D : $4(l/bt)$ for a prism, the dimension of the prism specimen (100×100×300) mm.

M : Mass of specimen (kg)

n' : fundamental longitudinal frequency (Hz)

This system provides the fundamental longitudinal frequency (n') from the Fast Fourier Transform (FFT). The FFT's maximum amplitude frequency value is applied to a time-domain signal collected by tapping the prism with a small, six mm-diameter hardened steel.



Figure 6. Non-Destructive Test Equipment (James Instruments)

ball. The specimen should be positioned on the test bed center support at the nodal point, as indicated in Fig.7, as only one nodal point is used for this test. The specimen is clamped using the clamping bar provided. The test has been done with a prism specimen (100×100×300) mm.

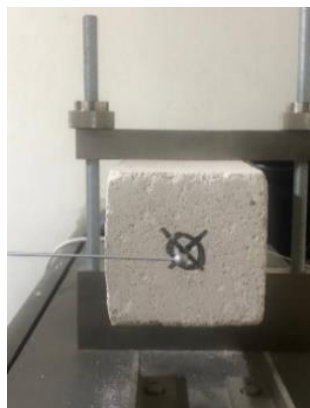


Figure 7. Testing of Longitudinal Resonance Frequency (James Instruments)

The test was done by placing the accelerometer on the center of the face of the prism; the accelerometer and prism must come into contact. The ends of the prism need to be minimally restrained for the free end to vibrate longitudinally. The support is kept in place by the knurled clamping screw, allowing the accelerometer to move freely and move along the rails until it contacts the specimen's center. The system showed the fundamental longitudinal frequency from the FFT that appeared on the screen.

The following equation was also used to calculate the value of E_c , including both their ρ and UPV values, in accordance with the standard CSN 73 1371 from [14].

$$E_c = \frac{\rho \times (UPV)^2 \times (1 + V_{dyn})(1 - 2V_{dyn})}{1 - V_{dyn}} \quad (9)$$

Where: E_c : Modulus of Elasticity,

ρ : Density

UPV: Ultrasonic Pulse Velocity,

V_{dyn} : Poisson's ratio

3.3.5 Poisson's Ratio (ν)

The test has been done with a prism Specimen (100×100×300) mm. The Poisson's ratio is depending a little on the dry density. As mentioned, the

torsional frequency mode test was done using non-destructive test equipment, James Instruments. The system obtained the fundamental torsional frequency (n'') from the FFT, which is applied to a time-domain signal acquired by tapping the prism with a small, six mm-diameter hardened steel ball. The system calculated the dynamic Poisson's ratio according to the equation[22]:

$$\nu = E/(2G) - 1 \quad (10)$$

Where:

$$G = B M (n'')^2 \quad (11)$$

ν : Poisson's ratio

G : dynamic modulus of rigidity

E : Dynamic modulus of elasticity

n'' : fundamental torsional frequency (Hz)

M : Mass of specimen (kg)

$$B = 4LR/A$$

$R = 1.183$ for prism,

A = cross-sectional area m^2

The test was done by putting the specimen in the equipment using the same method mentioned in the longitudinal frequency test. Then, using the ball, tap the prism, triggering the instrument, and a signal appears on the screen. Caution should be taken to apply just one solid impact in a specified spot, as illustrated in Fig.8. The system showed the fundamental torsional frequency from the FFT that appeared on the screen.



Figure 8. Testing of Torsional Resonance Frequency (James Instruments)

3.4 Shear Bond Test

The procedure to prepare the three specimens for the shear bond test was as follows:

- Using an electrical saw, the nominal AAC block with dimensions (200×200×600) mm was cut into three pieces with dimensions (200×200×200) mm.
- Preparing the mortars as mentioned before.
- Put the pieces of blocks in one raw, then a layer of mortar 10 mm thick between them.
- Confirm that the specimens with a steel frame are ready for testing.

The strength of masonry depends on the strength of the joining material; mortar strength is affected by the mechanical properties of AAC masonry. The specimens are shown in Fig. 9 below. To provide excellent shear conditions along the mortar joints, we have to bond the block surfaces well with a larger thickness of the mortar joints [23].

A direct testing technique named the triplet test was used to measure the shear bond strength of the AAC block and the mortar contact. AAC block masonry triplet specimen was used for one of each type of mortar to obtain the shear bond strength of the block mortar joints. It is clear from Fig. 9 below that a steel frame restrained the horizontal movement of the blocks, but the vertical movement was free for the specimens. The specimen was based horizontally on two supports in the middle of the side blocks and subjected to a vertical load at the center of the specimen. The load was applied gradually using the hydraulic jack with a capacity of 200 kN till the bond between the block and mortar joint failed; the tests reached their maximum load, at which point the execution was stopped.



a) Gypsum Specimen



b) Adhesive Specimen



c) Cement-Sand Specimen

Figure 9. Shear Bond Strength Test

The equation could estimate the shear bond strength:

$$\tau = \frac{V}{A} \quad (12)$$

where: τ : shear bond stress (MPa),

V : shear force (kN), which is equal to $P/2$,

A : contact area (mm)

4. Results and Discussion

The main findings are described in this section, and their importance and interpretation are explained in the discussion.

4.1 Results of Mechanical Properties

The mechanical properties of the AAC block and the mortars are listed in Table 7 below. These results are the average of three samples for each test.

Table 7. Results of Mechanical Properties

Specimen	$f'c$ (MPa)	Direct f_t (MPa)	Indirect f_t (MPa)	f_r (MPa)	E (MPa)	ν	Density kg/m ³
AAC Block	2.2	0.116	-	0.36	438.75	0.168	585
Experimental	2.93	0.296	-	0.732	-	-	-
Cement and sand mortar	18.55	1.875	1.02	2.344	3400	0.227	2071.7
Gypsum mortar	5.18	1.42	1.375	0.78	1100	0.17	1880
Adhesive mortar	9.4	3.25	1.496	1.28	1400	0.182	1560

The results showed that the compressive strength of cement-sand mortar was more than that of gypsum mortar and adhesive mortar by 72% and 49%, respectively. In addition, the direct tensile strength of cement-sand mortar was increased by 24% compared with gypsum and decreased by 73% compared with adhesive mortar. That means the tensile strength of adhesive material was more than others. The modulus of rupture, modulus of elasticity, and density also increased by (66% and 45%), (67% and 59%), and (9% and 25%) in cement-sand mortar rather than the gypsum and adhesive mortar, respectively.

Cement as a material is strong in compressive strength but weak in tensile strength, and this is what appeared in the results of cement-sand mortar. On the other hand, the increase in tensile strength in the adhesive mortar is explained by this material's distinctive structural composition, making it efficient in use with masonry blocks. The equations to calculate the mechanical properties of AAC blocks showed higher values than the experimental results in compressive strength, direct tensile strength, and modulus of rupture by (33, 155, and 103) %, respectively. This may explain why the equations were formulated on a larger sample size, so tests must always be performed on the specimens and not rely only on the equations' results.

4.2 Shear Bond Strength

Three specimens were tested to determine the shear bond strength for AAC block prisms. The

first specimen used cement mortar, the second used gypsum mortar, and the last used adhesive mortar. The results of the test are listed in Table 8.

Table 8. Results of Shear Bond Strength

Model	Type of Mortar	Failure Area (mm ²)	Load (V) (kN)	Shear Strength (MPa)
1	Cement	30000	2.5	0.043
2	Gypsum	27000	3	0.056
3	Adhesive	19000	3.8	0.1

The failure area is calculated by multiplying the mortar width by the crush depth in the mortar zone. The failure modes shown in Fig. 10 show that the crack starts almost at 50% of P_u at the bottom of the specimen due to the weakness of shear and flexural resistance between the AAC blocks and the bonding material under the neutral axis. Then, due to the increased loads, the crack turns into an inclined crack, causing flexural shear failure in the AAC above the neutral axis because of the high stress in this zone.



(a) Cement



(b) Gypsum



(c) Adhesive

Figure 10. Failure Pattern of Shear Bond

This mode of failure was observed in all the specimens. The difference between the three specimens was the failure crack depth according to the mortar type. The cement-sand mortar produced a higher crack depth along the block-mortar interface than the adhesive mortar, which cracked without sliding between AAC blocks. The results showed that the shear resistance of the model when using the adhesive mortar is higher than the shear resistance when using the rest of the bonding materials. The crack explains this began to tilt in the tension zone below the neutral axis, indicating that the bond strength between the blocks and the adhesive was higher against bending forces than other bond materials. Adhesive mortar showed superior tensile bond strength compared to cement-sand and gypsum mortars. This may be explained by better homogeneity of the adhesive mortar with AAC blocks. This

advantage may be reflected in full-sized masonry assemblies' shear and bending performance.

5. Conclusions:

AAC is encouraged because it is inexpensive, energy-efficient, and environmentally friendly, improves thermal performance, and provides building sound and fire insulation. Knowledge of construction materials' most critical mechanical properties is required for software-based or engineering design and analysis. In this work, attention was given to the construction materials utilized in AAC walls and the bonding and plastering mortars. The work estimated mechanical property values of AAC blocks, cement-sand mortar, gypsum, and adhesive mortar. The study dealt with the test procedure, approved specifications, and theoretical equations for calculating the properties of AAC blocks. Conducting practical tests with equations better to understand the mechanical property values and design requirements is always important. The results showed that the compressive strength value was higher in the cement-sand mortar compared to the gypsum and adhesive mortar.

On the other hand, the tensile strength of the adhesive was better than other materials. The adhesive mortar also showed superior performance in shear resistance, so it's recommended to use it in the AAC masonry. It was concluded that the bond strength between blocks improves by increasing the strength of the mortar, which in turn increases the adhesion at the block-mortar interface. It is useful to use a mortar with high tensile strength and consistency that gives more uniformity to the AAC blocks. The authors recommend testing larger-scale AAC assemblies, large sample-sizing with a results comparison of destructive and nondestructive tests, and numerical modeling to extend the experimental results and more parametric study.

Author Contribution Statement

Sarra'a Dhiya'a Jaafer carried out the experiments, discussed the experimental and theoretical results, designed the tables and figures, and wrote the manuscript.

Ashraf A. Alfeehan was involved in planning and supervising the work, contributing to the interpretation of the results and to the final writing of the manuscript.

Acknowledgments

The authors would like to thank Mustansiriyah University, Baghdad, Iraq, <https://www.uomustansiriyah.edu.iq>, for its support in the present work.

References

- [1] C. Fudge, F. H. Fouad, and R. E. Klingner, "Autoclaved Aerated Concrete," *Developments in the Formulation and Reinforcement of Concrete (Second Edition) Woodhead Publishing Series in Civil and Structural Engineering*, pp. 345–363, Jan. 2019, doi: <https://doi.org/10.1016/b978-0-08-102616-8.00015-0>
- [2] Ahmad et al., "A Step Towards Sustainable Concrete with Substitution of Plastic Waste in Concrete: Overview on Mechanical, Durability and Microstructure Analysis," *Crystals*, vol. 12, no. 7, p. 944, Jul. 2022, doi: <https://doi.org/10.3390/cryst12070944>
- [3] W. Emad, A. S. Mohammed, R. Kurda, K. Ghafor, L. Cavaleri, S. Qaidi, A.M.T. Hassan, P. G. Asteris, "Prediction of concrete materials compressive strength using surrogate models", *Structures*, vol. 46, pp. 1243-1267, 2022. <https://doi.org/10.1016/j.istruc.2022.11.002>.
- [4] O. F. Halici et al., "From Experiments To Seismic Design Rules For Structures Built With Reinforced Autoclaved Aerated Concrete Panels," *Ce/Papers*, vol. 2, no. 4, pp. 275–282, 2018, doi: <https://doi.org/10.1002/cepa.831>.
- [5] A. Raj, A. C. Borsakia, and U. S. Dixit, "Bond Strength Of Autoclaved Aerated Concrete (AAC) Masonry Using Various Joint Materials," *J. Build. Eng.*, vol. 28, p. 101039, 2020, doi: <https://doi.org/10.1016/j.jobbe.2019.101039>.
- [6] A. Raj, A. Ch, and B. Uday, "Compressive And Shear Bond Strengths Of Grooved AAC Blocks And Masonry," *Mater. Struct.*, vol. 8, 2019, doi: <https://doi.org/10.1617/s11527-019-1428-8>.
- [7] [4]J. A. Thamboo and M. Dhanasekar, "Characterisation of Thin Layer Polymer Cement Mortared Concrete Masonry Bond," *Construction and Building Materials*, vol. 82, pp. 71–80, May 2015, doi: <https://doi.org/10.1016/j.conbuildmat.2014.12.098>.
- [8] V. Alecci, M. Fagone, T. Rotunno, and M. De Stefano, "Shear Strength of Brick Masonry Walls Assembled With Different Types Of Mortar," *Constr. Build. Mater.*, vol. 40, pp. 1038–1045, 2013, <https://doi.org/10.1016/j.conbuildmat.2012.11.107>.
- [9] S. Barattucci, V. Sarhosis, A. W. Bruno, A. M. D'Altri, S. de Miranda, and G. Castellazzi, "An Experimental and Numerical Study on Masonry Triplets Subjected to Monotonic and Cyclic Shear Loadings," *Construction and Building Materials*, vol. 254, p. 119313, Sep. 2020, doi: <https://doi.org/10.1016/j.conbuildmat.2020.119313>.
- [10] G. Sarangapani, B. V. Venkatarama Reddy, and K. S. Jagadish, "Brick-Mortar Bond and Masonry Compressive Strength," *Journal of Materials in Civil Engineering*, vol. 17, no. 2, pp. 229–237, Apr. 2005, doi: [https://doi.org/10.1061/\(asce\)0899-1561\(2005\)17:2\(229\)](https://doi.org/10.1061/(asce)0899-1561(2005)17:2(229)).
- [11] S. H. Basha, Z.-X. Guo, and X. Xie, "Effect of Structural Bonding Patterns on Mechanical Characteristics of Clay Brick Masonry under Different Loadings Using Digital Image Correlation Technique," *Journal of Materials in Civil Engineering*, vol. 34, no. 11, Nov. 2022, doi: [https://doi.org/10.1061/\(asce\)jmt.1943-5533.0004457](https://doi.org/10.1061/(asce)jmt.1943-5533.0004457).
- [12] S. Andlun, "A Study on Material Properties of Autoclaved Aerated," Middle East Tech. Univ., p. 123, 2006.
- [13] [8]S. Aroni, *Autoclaved Aerated Concrete - Properties, Testing and Design*, 1st ed. London: CRC Press, 2004. Available doi: <https://doi.org/10.1201/9781482271195>.
- [14] [9]D. Kocac, R. Halamová, and B. Kucharczyková, "Determination of the Static Modulus of Elasticity of Cement Mortars in the Early Stage of Ageing," *MATEC Web of Conferences*, vol. 310, pp. 00029–00029, Jan. 2020, <http://doi.org/10.1051/mateconf/202031000029>.
- [15] A. Raj, A. C. Borsakia, and U. S. Dixit, "Evaluation of Mechanical Properties of Autoclaved Aerated Concrete (AAC) Block and its Masonry," *J. Inst. Eng. Ser. A*, vol. 101, no. 2, pp. 315–325, 2020, doi: <https://doi.org/10.1007/s40030-020-00437-5>.
- [16] ASTM, "Standard Specification for Autoclaved Aerated Concrete (AAC) 1," vol. i, no. Reapproved, pp. 1–7, 2017, doi: <https://doi.org/10.1520/C1693-11R17.2>.
- [17] ASTM, "Standard Test Method for Laboratory Determination of Pulse Velocities and Ultrasonic Elastic Constants of Rock," vol. 14, 2000.
- [18] W. Equipment, S. Molds, M. Chamber, T. Machine, and T. Clips, "Standard Test Method for Tensile Strength of Chemical-Resistant Mortar, Grouts, and Monolithic Surfacing," vol. i, no. Reapproved 2008, pp. 3–6, 2009.
- [19] U. M. E. Cancino, "Behavior of Autoclaved Aerated Concrete Shear Walls With Low-Strength AAC," MSc thesis, The University of Texas at Austin. December, 2003.
- [20] N. Narayanan and K. Ramamurthy, "Structure and Properties of Aerated concrete: a Review," *Cement and Concrete Composites*, vol. 22, no. 5,

pp. 321–329, Oct. 2000, [https://doi.org/10.1016/S0958-9465\(00\)00016-0](https://doi.org/10.1016/S0958-9465(00)00016-0).

- [21] F. Gökmen, “*Seismic Behavior of Autoclaved Aerated Concrete Reinforced Vertical Panel Buildings*,” a Thesis Submitted To The Graduate School Of Natural And Applied Sciences Of Middle East Technical University, 2017. Available: <http://etd.lib.metu.edu.tr/upload/12621425/index.pdf>
- [22] ASTM, “*Standard Test Method for Fundamental Transverse, Longitudinal, and Torsional Resonant Frequencies of Concrete Specimens*,” pp. 1–7, 2019. <https://doi.org/10.1520/C0215-19>
- [23] F. Li, G. Chen, Y. Zhang, Y. Hao, and Z. Si, “Fundamental Properties and Thermal Transferability of Masonry Built by Autoclaved Aerated Concrete Self-Insulation Blocks,” *Materials*, vol. 13, no. 7, p. 1680, Apr. 2020, doi: <https://doi.org/10.3390/ma13071680>.